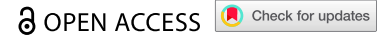


ORIGINAL RESEARCH



A mechanism of IL-34-induced resistance against cytotoxic anti-cancer therapies such as radiation by X-ray and chemotherapy by Oxaliplatin

Nanumi Han, Haruka Wada, Takuto Kobayashi, Ryo Otsuka, and Ken-Ichiro Seino 

Division of Immunobiology, Institute for Genetic Medicine, Hokkaido University, Sapporo, Japan

ABSTRACT

Interleukin-34 (IL-34) has been known as a factor that is involved with tumor progression and therapeutic resistance. However, there are limitations to addressing the mechanism of how IL-34 induces therapeutic resistance. Here, we show a mechanism of IL-34-induced resistance against cytotoxic anti-cancer therapies such as radiotherapy using X-ray and chemotherapy by Oxaliplatin. This research demonstrates that IL-34 immunologically changes the tumor microenvironment after treatments with radiation or chemotherapeutic agents such as oxaliplatin. We identified the changes in immune cells using flow cytometry and immunofluorescent (IF) staining, which are up-regulated upon the existence of IL-34. Overall, these findings demonstrate the possibility of IL-34 blockade as a novel combination therapy for cancer.

ARTICLE HISTORY

Received 28 March 2023
Revised 6 July 2023
Accepted 15 July 2023

KEYWORDS

Chemotherapy; IL-34; immunosuppression; radiotherapy; therapeutic resistance

Introduction

Since the discovery of IL-34 as a ligand of CSF-1 R, which is classically known as a receptor of CSF-1,¹ several reports have addressed the relationships between IL-34 and pathological conditions.² Among these reports, there are many reports that various types of cancer express IL-34, and reports demonstrating the correlation between IL-34 and poor prognosis in cancer.^{3,4} Besides, several reports suggested that IL-34 has related to metastasis and tumor progression.^{5,6} Specifically, a report shows IL-34 promotes gastric cancer progression and invasion via EMT induction.⁷ In osteosarcoma, it shows that IL-34 promotes tumor progression and metastatic process inducing angiogenesis and macrophage recruitment.⁸ Further, there are reports suggesting IL-34 expression induces resistance to Oxaliplatin in colorectal cancer.⁶ In the case of immune checkpoint inhibitors such as anti-PD-1 antibodies, we suggested that IL-34 expression could contribute to therapeutic resistance in a clinical case.⁹ Following this suggestion, our recent report indicated that IL-34 induces immunotherapeutic resistance reducing pro-inflammatory macrophages characterized as Nos2 positive. In sequence, we investigated the efficacy of IL-34 blockade in a patient-derived xenograft model with immunotherapy, and the results showed the possibility of IL-34 blockade as a novel therapy.¹⁰ For these reasons, IL-34 has been suggested as a factor that worsens tumor prognosis and induces therapeutic resistance. Although a mechanism by which IL-34 induces resistance to ICBs has been partially elucidated, the mechanism of chemotherapeutic resistance with oxaliplatin remains unclear. In the case of radiotherapy, which is the main treatment modality, IL-34 may induce therapeutic resistance, but the relation between IL-34 expression and therapeutic resistance has not yet been investigated. It is considered necessary to

investigate the effect of IL-34 on other therapies such as radiotherapy or chemotherapy. Therefore, we investigated the effect of IL-34 on radiotherapy and chemotherapy using *in vivo* model with *Il34* knock-out cancer cells.

Materials and methods

Mice



All experimental procedures were approved by the Hokkaido University Animal Care Committee (Approval number:19-0094). Six to eight-week-old female BALB/c, BALB/c nu/nu mice were purchased from Japan SLC, Inc. The mice were maintained under specific pathogen-free conditions in the animal facility at Hokkaido University.


Cell lines and culture

Murine colorectal carcinoma cell line CT26 and mammary carcinoma cell line 4T1 were purchased from ATCC (Manassas). Mock 4T1, *Il34*^{KO} 4T1, *Il34*^{KO} CT26 and *Il34*^{OE} CT26 cell lines were generated as previously reported (6). The cell lines were maintained in RPMI-1640 (Fujifilm Wako Pure Chemical Industries). All culture media were supplemented with 10% fetal bovine serum (Sigma), 1% Penicillin/Streptomycin (Nacalai Tesque), and 1% Non-Essential Amino Acid (Nacalai Tesque). All cells were maintained in a humidified incubator with 5% CO₂ at 37°C.

Cell viability assay

Mock 4T1 and *Il34*^{KO} 4T1 cells were irradiated 4 Gy for three days with the same fractions as *in vivo* model. Cells were placed

CONTACT Ken-ichiro Seino  seino@igm.hokudai.ac.jp  Division of Immunobiology, Institute for Genetic Medicine, Hokkaido University, Kita-15, Nishi-7, Sapporo 060-0815, Japan

 Supplemental data for this article can be accessed online at <https://doi.org/10.1080/2162402X.2023.2238499>

© 2023 The Author(s). Published with license by Taylor & Francis Group, LLC.

This is an Open Access article distributed under the terms of the Creative Commons Attribution-NonCommercial License (<http://creativecommons.org/licenses/by-nc/4.0/>), which permits unrestricted non-commercial use, distribution, and reproduction in any medium, provided the original work is properly cited. The terms on which this article has been published allow the posting of the Accepted Manuscript in a repository by the author(s) or with their consent.

at 450 mm, and the irradiation condition was 150 kV, 5 mA with 1.0 mm Aluminum and 0.2 mm copper filter at a dose rate of 0.4 Gy/min. *Il34^{KO}* CT26 and *Il34^{OE}* CT26 were treated with 0, 1.2, 8.8, and 100 μ M of OXP and cultured three days. To assess cell viability, MTT assay was performed using MTT Cell count kit (Nacalai Tesque). Absorbance at a test wavelength of 570 nm and a reference wavelength of 650 nm was measured by using a Multiskan FC (Thermo Fisher Scientific). Cell proliferations were observed up to 4 days.

Radiotherapy model

2×10^5 Mock 4T1 and *Il34^{KO}* 4T1 cells were inoculated subcutaneously (s.c.) into the right flank of syngeneic BALB/c or BALB/c nu/nu female mice. Only tumor tissue was irradiated three times at 4 Gy of X-ray 10 days after inoculation. Irradiation was performed with a HITACHI X-ray Irradiation Apparatus MBR-1520 R-04. For local tumor irradiation, anesthetized mice were placed at 450 mm (the focal distance). Irradiation condition was 150 kV, 5 mA with 1.0 mm Aluminum and 0.2 mm copper filter at a dose rate of 0.4 Gy/min. The rest of the body was shield by 1 cm of lead. The mice were anesthetized by a mixture of three drugs: medetomidine (Domitor[®] Nippon Zenyaku Kogyo Co., Ltd.), midazolam (Dormicum[®], Astellas Pharma Inc.), and butorphanol (Vetorphale[®], Meiji Seika Kaisha, Ltd., Japan). Mixing ratio of drugs were as follows: Medetomidine: 0.75 ml (3.75%), Midazolam: 2 ml (10%), Butorphanol: 2.5 ml (12.5%), 0.9% saline: 14.75 ml (73.75%). 20 μ l of mixture was injected intraperitoneally. Tumors were measured twice a week using caliper and volumes were calculated by the formula: length \times width \times height \times $\pi/6$.

Chemotherapy model

2×10^5 *Il34^{KO}* CT26 and *Il34^{OE}* CT26 cells were inoculated subcutaneously (s.c.) into the right flank of syngeneic BALB/c female mice. Mice were randomly divided into two groups 7 days after tumor inoculation, and injected intraperitoneally with OXP (10 mg/kg). The dose of L-OHP was every 3 days until day 19. Tumors were measured twice a week using caliper and volumes were calculated by the formula: length \times width \times height \times $\pi/6$.

Antibody injections

CD4⁺ T cells were depleted with monoclonal anti-CD4 (clone GK1.5) and CD8⁺ T cells were depleted with monoclonal anti-CD8 (clone 53-6.72) antibodies. ChromPure Rat IgG, whole molecule (Jackson Immuno Research) was used as control IgG. For CSF-1 R inhibition, 200 μ g of anti-CSF-1 R (Bio X Cell) antibody was used. In the case of radiotherapy, the antibodies were injected intraperitoneally on day 7 and day 9 after inoculation of tumor cells (1 and 3 days before irradiation). In the case of chemotherapy, antibodies were injected intraperitoneally three and one day before inoculation of tumor cells. Respective antibodies were purified in our laboratory. For immune checkpoint inhibition, 250 μ g of anti-PD-1 (RMP1-14) antibody was injected intraperitoneally on day 5, 7, 9, and

12. Anti-PD-1 antibody was kindly provided by Dr. Hideo Yagita (Juntendo University).

Isolation of tumor-infiltrating immune cells from solid tumor

Isolation of tumor-infiltrating immune cells from solid tumors was performed by using BD Horizon™ Dri Tumor & Tissue (BD Biosciences). The recovered tumor-infiltrating cells were used as samples for flow cytometry.

Flow cytometry

Collected tumor infiltrating immune cells were washed and blocked Fc receptor by purified anti-mouse CD16/CD32 (TONBO biosciences) and stained with 4',6-diamidino-2-phenylindole (DAPI, Cayman Chemical Company) and the antibodies against following molecules; Arg1, CD3 ϵ , CD4, CD8, CD11b, CD11c, CD45, F4/80, IFN- γ , and Nos2. Transcription Factor staining Buffer Set (Invitrogen™) was used for intracellular staining. Data were acquired using BD FACSCelesta (BD Biosciences) flow cytometer, and analyzed using FlowJo (BD Biosciences, USA) software. Following is detailed information on antibodies. Purified anti-mouse CD16/CD32 (2.4G2) (TONBO bioscience), Anti-human/mouse Arginase1 (A1exF5) PE (Invitrogen™), Anti-mouse CD3 ϵ (145-2C11) APC (BioLegend), Anti-mouse CD4 (RM4-5) APC-Cy7 (BioLegend), Anti-mouse CD8 α (53-6.7) PerCP-Cy5.5 (BioLegend), Anti-mouse CD11b (M1/70) Pacific blue (BioLegend), Anti-mouse CD11c (N418) PerCP-Cy5.5 (BioLegend), Anti-mouse CD45 (30-F11) Brilliant Violet 650™ (BioLegend), Anti-mouse F4/80 (BM8) APC (BioLegend), Anti-mouse IFN- γ (XMG1.2) PE (BD Biosciences), Anti-mouse iNOS (CXNFT) PE (Invitrogen™).

Immunofluorescent staining

Opal 4-color fluorescent IHC kit (Perkin-Elmer) was used. Tumor sections were objectively judged by two independent researchers at 200 \times magnification for each section. More than seven tumor areas in each section were randomly selected for evaluation. Zeiss software was used for quantification of immunofluorescent staining. Following is detailed information on antibodies. Purified anti-mouse CD8 α (5H10-1) (BioLegend), Anti-mouse IFN- γ (XMG1.2) PE (BD Biosciences), Purified anti-mouse F4/80 (BM8) (BioLegend), LEAF IL-12/IL-23 p40 (C17.8) (BioLegend).

Quantitative PCR analysis

Total RNAs were extracted using TRIsure reagent (NIPPON Genetics Co., Ltd., Japan). 1 μ g of total RNAs was cDNA was synthesized using ReverTra Ace[®] qPCR RT Master Mix (TOYOBO, Japan). Quantitative PCR was performed on cDNA using KAPA SYBR[®] FAST qPCR Master Mix (2X) ABI Prism[®] (NIPPON Genetics Co., Ltd., Japan) on a StepOnePlus Real-Time PCR System (Thermo Fisher Scientific, MA, USA). The following primers were used for RT-qPCR. *Gzmb* (forward: 5'-ACTCTTGACGCTGGGACCTA-3' and reverse: 5'-

AGTGGGGCTTGACTTCATGT-3'), *Tnfa* (forward: 5'-TTCTATGGCCCAGACCCTCA-3' and reverse: 5'-CTTGGTGGTTTGCTACGACG-3'), *Gapdh* (forward: 5'-CATGGCCTTCCGTGTTCCCTA-3' and reverse: 5'-GCGGCACGTCAGATCCA-3')

Enzyme-linked immunosorbent assay (ELISA)

The production of HMGB-1 in cell lines after X-ray irradiation or OXP addition were measured with ELISA. Cell lysates were collected at 48 h after the irradiation or OXP addition. The HMGB-1 contents were measured with Mouse/Rat HMGB1 ELISA Kit (ARG81310, arigo Biolaboratories Corp.,)

Statistics

Statistical analysis was performed with JMP® 14 (SAS Institute Inc.). Significance was determined by Student's t-test, Tukey's multiple comparison test. p-Value was considered statistically significant when < 0.05 .

Results

As previously reported, we indicated that IL-34 impedes the anti-tumor effect inducing monocyte to immune suppressive macrophage in immune checkpoint blockade treated tumor microenvironment. We examined the possibility that IL-34 derives resistance in radiotherapy (RT) and chemotherapy from this mechanism analysis. Mice were inoculated with *Il34* knock-out mouse breast cancer 4T1 (*Il34*^{KO} 4T1)

subcutaneously (s.c.) into the right flank. We utilized the same cell lines, *Il34*^{KO} 4T1, and its control, mock-transfected 4T1 (Mock 4T1), in our previous report.¹⁰ The tumor tissues were irradiated three times at 4 Gy 10 days after inoculation (Figure 1a). The dose and amount of radiation treatment were determined by referring to the previous reports.¹¹ The volume of irradiated mock 4T1 (Mock + RT) and *Il34*^{KO} 4T1 (*Il34*^{KO} + RT) tumors markedly reduced on day 12 after irradiations compared to non-irradiated tumors (Mock and *Il34*^{KO}). Interestingly, the volume of *Il34*^{KO} + RT decreased significantly compared to the Mock + RT. Furthermore, *Il34*^{KO} + RT showed the smallest size after the treatment. Meanwhile, no significant differences were found between non-irradiated mock 4T1 and *Il34*^{KO} 4T1 (Figure 1b). From this result, we examined whether the sensitivity of irradiation treatment is altered in Mock 4T1 which produces IL-34 compared to *Il34*^{KO} 4T1. The cultured cells *in vitro* were irradiated with the same fractions as *in vivo* model and analyzed the survival by MTT assay. Despite a decreased survival by irradiation in Mock and *Il34*^{KO} 4T1, there was no significant difference between Mock and *Il34*^{KO} 4T1 (Figure 1c). These finding suggests that IL-34 induces resistance against radiotherapy and the anti-tumor effect improves only in radiotherapy-treated conditions in IL-34-deficient tumors. From the perspective of cancer cells, there are two possible ways to induce resistance against treatment in the tumor microenvironment through cytokine secretion. One is the way to survive through the autocrine pathway, and the other is through the paracrine pathway. There is a report that IL-34 works in both autocrine and paracrine in the human lung cancer cell A549 model which shows chemo-therapeutic

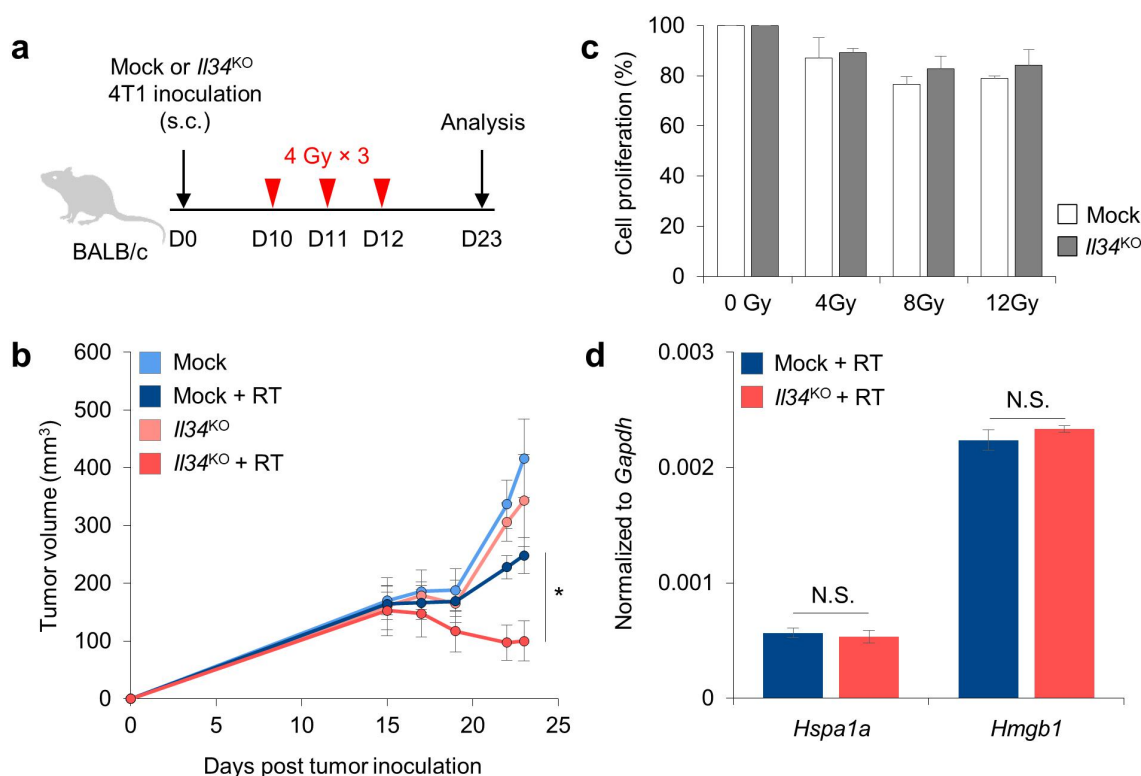


Figure 1. Evaluation of the possibility that IL-34 derives resistance in RT. (a) the timeline of inoculation, irradiation, and analysis for radiotherapy. (b) Tumor volume of BALB/c mice until day 23 with mean \pm SEM ($n = 6$ /group) (c) the percentage of surviving cells with mean \pm SEM ($n = 3$ /cell line) (d) Relative *Hspa1a* and *Hmgbl* mRNA expression by qPCR with mean \pm SEM ($n = 3$ /group). * $P < 0.05$; Tukey's multiple comparison test, N.S., Not significant.

resistance.¹² So, the CSF-1 R expressions on irradiated cells were analyzed using flow cytometry to determine the possibility of survival mediating the autocrine pathway. There were no expression changes of CSF-1 R on irradiated mock 4T1 and *Il34*^{KO} 4T1 as compared with non-irradiated mock 4T1 and *Il34*^{KO} 4T1 (data not shown). This result suggests that survival is maintained by the paracrine pathway rather than the autocrine pathway. Damage-associated molecular patterns (DAMPs) such as HMGB1 and Hsp70 are a component of damaged or dying cells by radiotherapy or chemotherapy. DAMPs are known as the factor that induces immunogenic cell death (ICD), which induces anti-cancer reaction through antigen presentation.¹³ To elucidate the relationship between ICD and therapeutic mechanisms in IL-34-deficient tumors, we examined the expression of representative DAMPs, Hsp70 and HMGB1, using quantitative PCR. As a result, there were no differences in *Hspa1a* and *Hmgb1* expression between Mock + RT and *Il34*^{KO} + RT (Figure 1d). Similar to the qPCR results, HMGB-1 protein expressions in Mock + RT and *Il34*^{KO} + RT were confirmed by ELISA (Supplementary figure S1a). We utilized nude mice to clarify immune system contributes to the anti-tumor effect on IL-34-deficient tumors in RT. Wildtype BALB/c (WT) mice, nude mice (Nu/Nu), and their control (Nu/+) mice were inoculated with *Il34*^{KO} 4T1 and irradiated in as same as in the previous experiment (4 Gy × 3) (Figure 2a). The tumor volume significantly increased in nude mice compared to control mice (Figure 2b). It indicates that the anti-tumor effect on IL-34-deficient tumors arose from the existence of T cells. Normal mice were treated with anti-CD4 or anti-CD8 antibodies to specify which type of cell induces an anti-tumor effect by deleting CD4⁺ or CD8⁺ T cells. The

antibodies were injected three days and a day before the beginning of the irradiation (Figure 2c). Anti-CD8 antibody injected mice showed significantly increased tumor volume compared to control IgG and anti-CD4 antibody injected mice. However, there was no significant difference between control IgG and anti-CD4 antibody injected mice (Figure 2d). The result implies that CD8⁺ T cells play a key role in the anti-tumor effect on IL-34-deficient tumors. Since the results suggest that T cells participate in the anti-tumor effect on IL-34-deficient tumors, we extended the investigation to determine the characteristics of infiltrating immune cells in the tumor microenvironment. We collected the tumors of each group on day 23 after inoculation (11 days later of irradiation) (Figure 1a) and analyzed the proportion of infiltrating immune cells into tumors by flow cytometry. We classified the infiltrating immune cells into four types; CD4⁺, CD8⁺ T cell, macrophage, and dendritic cell. Briefly, the infiltrating immune cells into tumor tissues were discriminated by CD45 expression. CD45⁺ cells were gated into CD3 as T cells and CD11b as myeloid cells. The population of CD4⁺ T cells decreased, and CD8⁺ T cells increased significantly in the irradiated groups compared to non-irradiated groups. Interestingly, there was no significant difference in the percentages of CD4⁺ and CD8⁺ T cells in tumor tissues between Mock + RT and *Il34*^{KO} + RT groups (Figure 3a). The population of macrophages discriminated by F4/80 increased significantly in the irradiated groups compared to non-irradiated groups. However, as with a result of T cells, there was no significant difference in the percentages of macrophages in tumor tissues between Mock + RT and *Il34*^{KO} + RT groups (Figure 3b). Although there was no difference in the number of immune cells after RT, we investigated

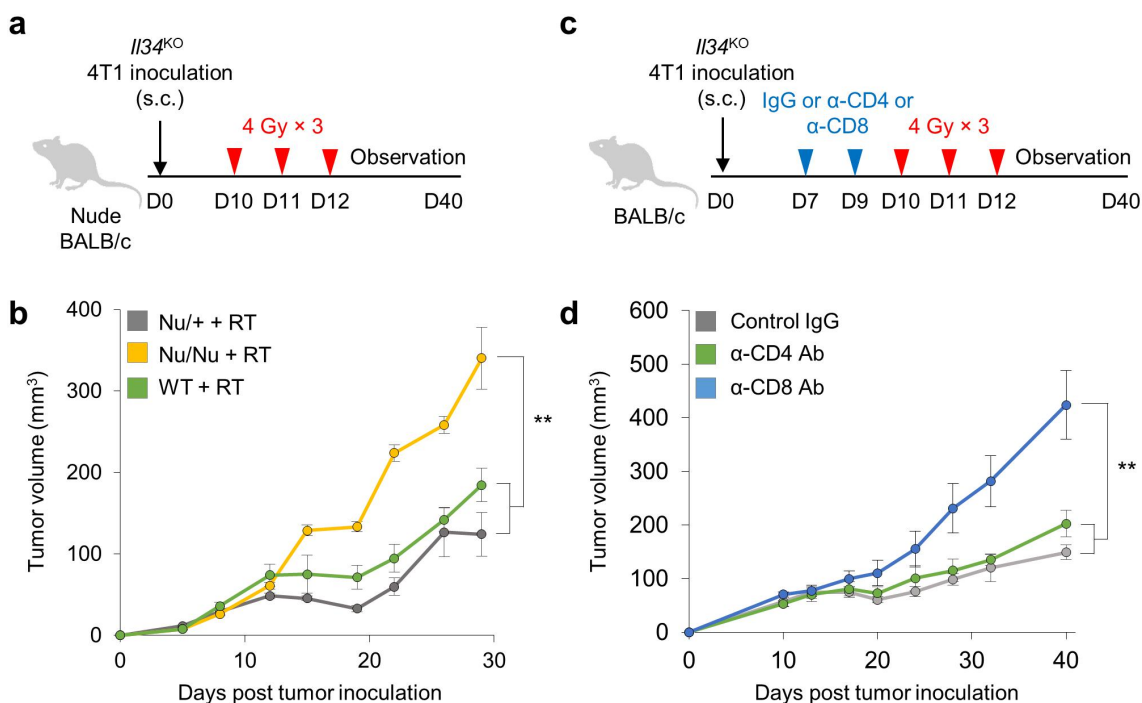


Figure 2. Analysis of the contribution of the immune system to anti-tumor effects in IL-34-deficient tumor. (a) the timeline of inoculation, irradiation, and analysis for radiotherapy in nude mice (Nu/Nu), the control of nude mice (Nu/+), and wildtype mice (WT). (b) Tumor volume of nude mice until day 29 with mean ± SEM ($n = 6$ /group) (c) the timeline of anti-CD4 or anti-CD8 antibody injection, inoculation, irradiation for radiotherapy. (d) Tumor volume of antibody injected BALB/c mice until day 23 with mean ± SEM ($n = 6$ /group). ** $P < 0.01$; Student's t-test (b), Tukey's multiple comparison test (d), N.S., Not significant.

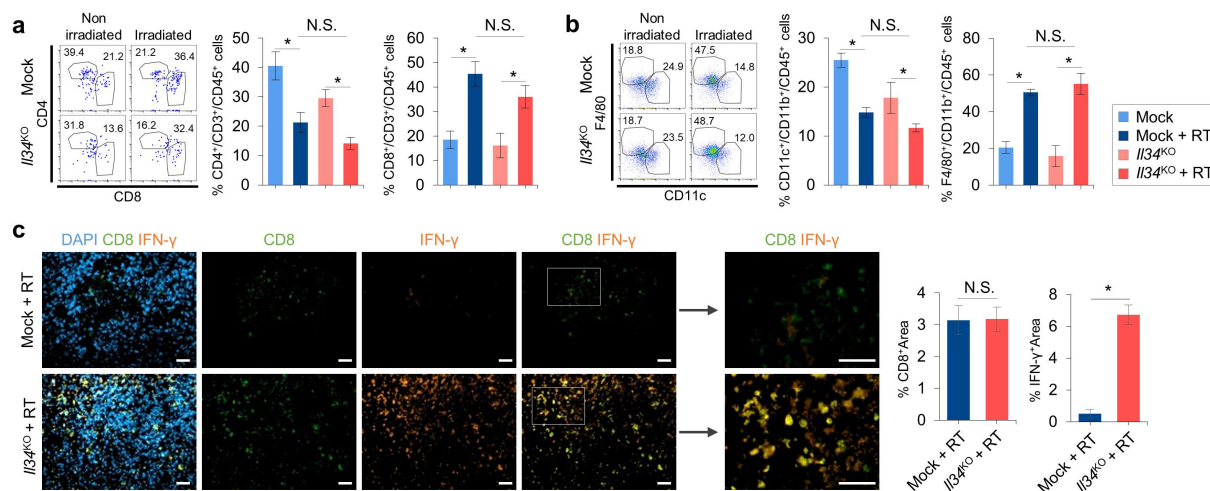


Figure 3. Characterization of immune cells in IL-34-deficient and IL-34-expressing tumor microenvironment after RT. (a) Representative flow cytometry plots of T cells in tumor of *Il34*^{KO} and Mock 4T1 before and after radiotherapy with mean \pm SEM ($n = 6$ /group). (b) Representative flow cytometry plots of dendritic cells and macrophages in tumors of *Il34*^{KO} and Mock 4T1 before and after radiotherapy with mean \pm SEM ($n = 6$ /group). (c) Representative images of IF staining of *Il34*^{KO} and Mock 4T1 after irradiation. Bar graphs show the percentage of CD8⁺ (left) and IFN⁺ (right) areas with mean \pm SEM ($n = 10$ /group). Scale bar: 20 μ m, * $P < 0.05$; Tukey's multiple comparison test, Student's t-test (c), N.S., Not significant.

the characteristics of T cells and macrophages in the tumor microenvironments because there may be differences in the function of immune cells. At first, we conducted immunofluorescent staining to verify the characteristics of CD8⁺ T cells. There was no change in the appearance of CD8⁺ T cells between Mock + RT and *Il34*^{KO} + RT groups as the same result with flow cytometry. However, the IFN- γ ⁺ area significantly increased in *Il34*^{KO} + RT (Figure 3c). This result suggests that T cell, which has an anti-tumor function, rose in the irradiated IL-34-deficient tumor. In our previous report, we suggested IL-34 induces therapeutic resistance regulating the Nos2 expression of macrophages in immunotherapy.¹⁰ So, we examined the Arg1 and Nos2 expression in macrophages using flow cytometry. Unlike the previous report, there was no difference in Arg1 (Figure 4a) and Nos2 expression between Mock + RT and *Il34*^{KO} + RT groups (Figure 4b). In sequence, we investigated the expression of IL-12 because it stimulates the production of IFN- γ and TNF- α from T cells.¹⁴ As a result, there was a significant increase of IL-12⁺ macrophages in *Il34*^{KO} + RT compared to Mock + RT (Figure 4c). In IF staining, there was no change in the appearances of macrophages between Mock + RT and *Il34*^{KO} + RT, and the same result with flow cytometry. However, the IL-12⁺ area significantly increased in *Il34*^{KO} + RT (Figure 4d). The only IL-12 expressing area rose in *Il34*^{KO} + RT with F4/80⁺ IL-12⁺ co-expression area compared to Mock + RT. And we also found that there were significant increases in *Gzmb* and *Tnfa* expression in *Il34*^{KO} + RT from the qPCR result (Figure 4e). From a therapeutic point of view, the blockade of CSF-1 R has a possibility to mimic the *Il34*^{KO} phenotype, subsequently, CSF-1 R inhibition was conducted. To compare the effect of CSF-1 R inhibition on IL-34 expressing tumor, the only mice which are inoculated by mock 4T1 were injected with anti-CSF-1 R antibody three and a day before irradiation start and tumor growth was observed until day 29 (Figure 5a). As expected, the Mock + α -CSF-1 R + RT group showed the anti-tumor effect as similar to *Il34*^{KO} + RT group while the Mock + α -CSF-1 R group does not

(Figure 5b). Further to this, the combination therapy with immune checkpoint antibody and X-ray irradiation was conducted. Anti-PD-1 antibody was injected on days 5, 7, 9, and 12 with irradiation on days 10, 11, and 12 (Figure 5c). Both groups show similar or smaller tumor volumes compared to Mock + RT and *Il34*^{KO} + RT and, on day 29, there was a difference between Mock + α -PD-1 + RT and *Il34*^{KO} + α -PD-1 + RT (Figure 5d). In chemotherapy, resistance to treatment was also a problem in some cases, and it is considered that there might be involvement of IL-34. Therefore, the effect of IL-34 in chemotherapy was continuously investigated according to the results of changes in the characteristics of immune cells in the IL-34-deficient tumor microenvironment after radiotherapy. First, we examined the possibility that IL-34 derives resistance in chemotherapy with the schedule shown in Figure 6a. We injected oxaliplatin (OXP) into the intraperitoneal five times after inoculation until day 19. The dose and amount of OXP treatment were determined by referring to the previous reports.¹⁵ The only volume of OXP-treated *Il34*^{KO} CT26 (*Il34*^{KO} + OXP) tumors markedly reduced from day 10 to day 19 (Figure 6b). Next, we examined whether the anti-tumor effect in *Il34*^{KO} + OXP is related to CD8⁺ T cells using the anti-CD8 antibody. Control IgG and anti-CD8 antibody injected mice 1 and 3 days before the inoculation of *Il34*^{KO} CT26, the OXP injections were conducted the same with Figure 6c. Treatment effect on *Il34*^{KO} CT26 by OXP was canceled in the anti-CD8 antibody injected group (Figure 6d). The cultured cells in vitro were administrated OXP for four concentrations and analyzed the survival by MTT assay. Despite a decreased survival by high concentration in *Il34*^{OE} and *Il34*^{KO} CT26, there was no significant difference (Figure 6e). As in the radiation experiment, HMGB-1 expression in *Il34*^{OE} + OXP and *Il34*^{KO} + OXP was examined by ELISA, and the expression was confirmed (Supplementary Figure S1b). Next, we collected the tumors of each group on day 19 after inoculation and analyzed the proportion of infiltrating immune cells into tumors by flow cytometry

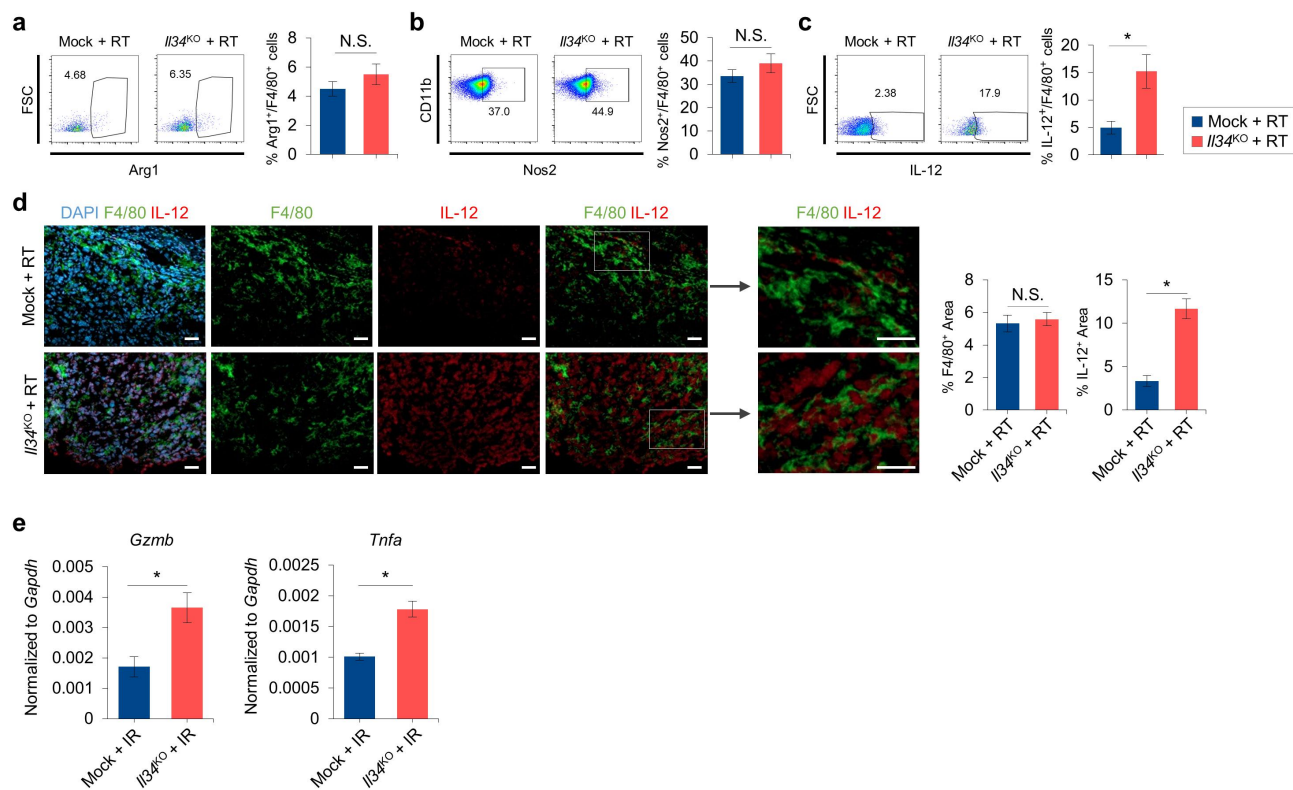


Figure 4. Characterization of macrophages in IL-34-deficient and IL-34-expressing tumor microenvironment after RT. (a) Representative flow cytometry data showing Arg1, Nos2, and IL-12 expression of macrophages in tumors of *Il34*^{KO} and Mock 4T1 after radiotherapy with mean \pm SEM ($n = 4$ /group). (b) Representative flow cytometry data showing Arg1, Nos2, and IL-12 expression of macrophages in tumors of *Il34*^{KO} and Mock 4T1 after radiotherapy with mean \pm SEM ($n = 4$ /group). (c) Representative flow cytometry data showing Arg1, Nos2, and IL-12 expression of macrophages in tumors of *Il34*^{KO} and Mock 4T1 after radiotherapy with mean \pm SEM ($n = 4$ /group). (d) Representative images of if staining of *Il34*^{KO} and Mock 4T1 after irradiation. Bar graphs show the percentage of F4/80⁺ (left) and IL-12⁺ (right) areas with mean \pm SEM ($n = 10$ /group). (e) Relative *Gzmb* and *Tnfa* mRNA expression by qPCR with mean \pm SEM ($n = 3$ /group). Scale bar: 20 μ m, * $P < 0.05$; Student's t-test, N.S., Not significant.

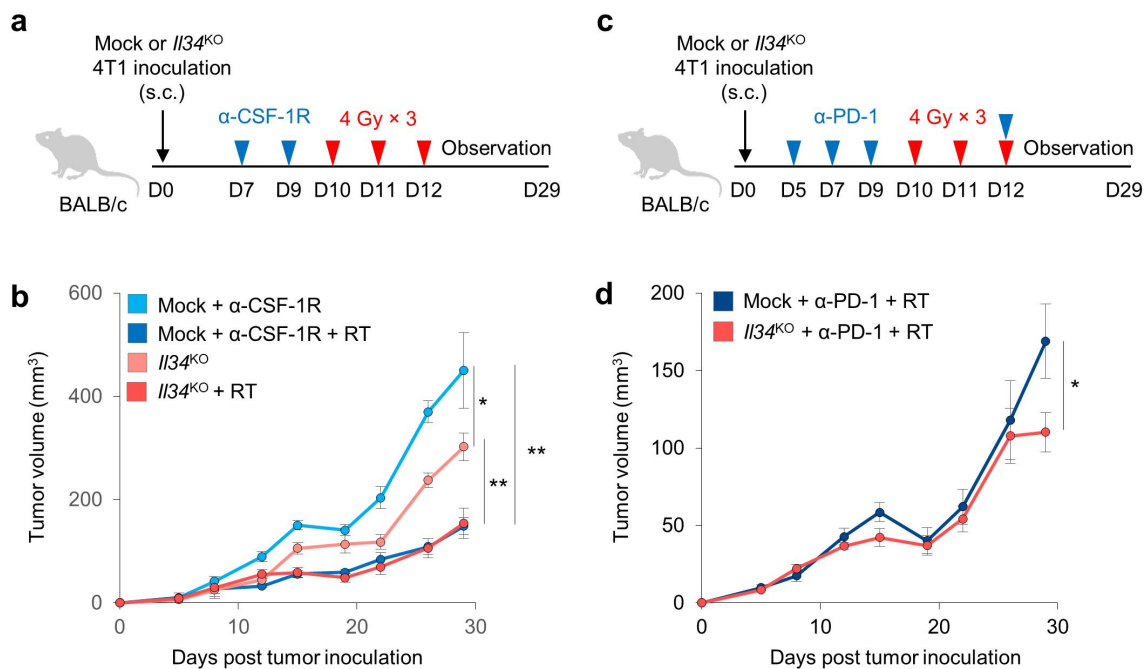


Figure 5. Evaluation of the possibility of improved treatment efficacy by CSF-1 R inhibition and anti-PD-1 antibody in RT. (a) the timeline of inoculation, irradiation, injection of anti-CSF-1 R antibody and analysis for radiotherapy. (b) Tumor volume of BALB/c mice until day 29 with mean \pm SEM ($n = 6$ /group) (c) the timeline of inoculation, irradiation, injection of anti-PD-1 antibody and analysis for radiotherapy. (d) Tumor volume of BALB/c mice until day 29 with mean \pm SEM ($n = 6$ /group) * $P < 0.05$, ** $P < 0.01$; Tukey's multiple comparison test, N.S., Not significant.

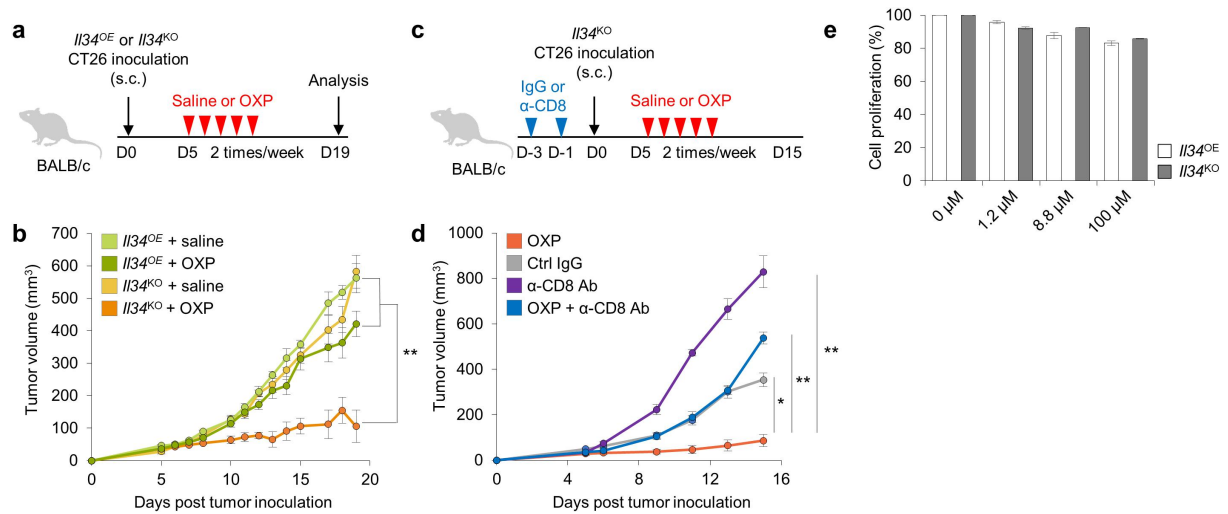


Figure 6. Evaluation of the possibility that IL-34 derives resistance in OXP treatment. (a) the timeline of inoculation, administration of OXP, and analysis for chemotherapy. (b) Tumor volume of BALB/c mice until day 19 with mean \pm SEM ($n = 6$ /group). (c) the timeline of anti-CD4 or anti-CD8 antibody injection, inoculation, and administration of OXP for chemotherapy. (d) Tumor volume of antibody injected BALB/c mice until day 15 with mean \pm SEM ($n = 6$ /group). (e) the percentage of surviving cells with mean \pm SEM after OXP addition ($n = 3$ /cell line). * $P < 0.05$, ** $P < 0.01$; Tukey's multiple comparison test, N.S., Not significant.

(Figure 6a). We classified the infiltrating immune cells into four types same as the analysis of radiotherapy. In the case of T cells, there was no significant difference in the percentages of CD4⁺ T cells in tumor tissues between the *Il34^{OE}* + OXP and *Il34^{KO}* + OXP. And the population of CD8⁺ T cells significantly increased in *Il34^{KO}* + OXP compared to *Il34^{OE}* + OXP (Figure 7a). There was no difference population of IFN- γ cells in the tumor microenvironment (data not shown). In

the case of myeloid cells, the macrophage population discriminated by F4/80 showed no differences between groups. Also, the DC population discriminated by CD11c showed no differences between groups (Figure 7b). So, we investigated the population of immuno-suppressive Arg1⁺ macrophages in the tumor microenvironment. Unlike the analysis of the radiotherapy sample (Figure 4a), Arg1⁺ macrophages significantly decreased in *Il34^{KO}* + OXP (Figure 7c). But there was the same

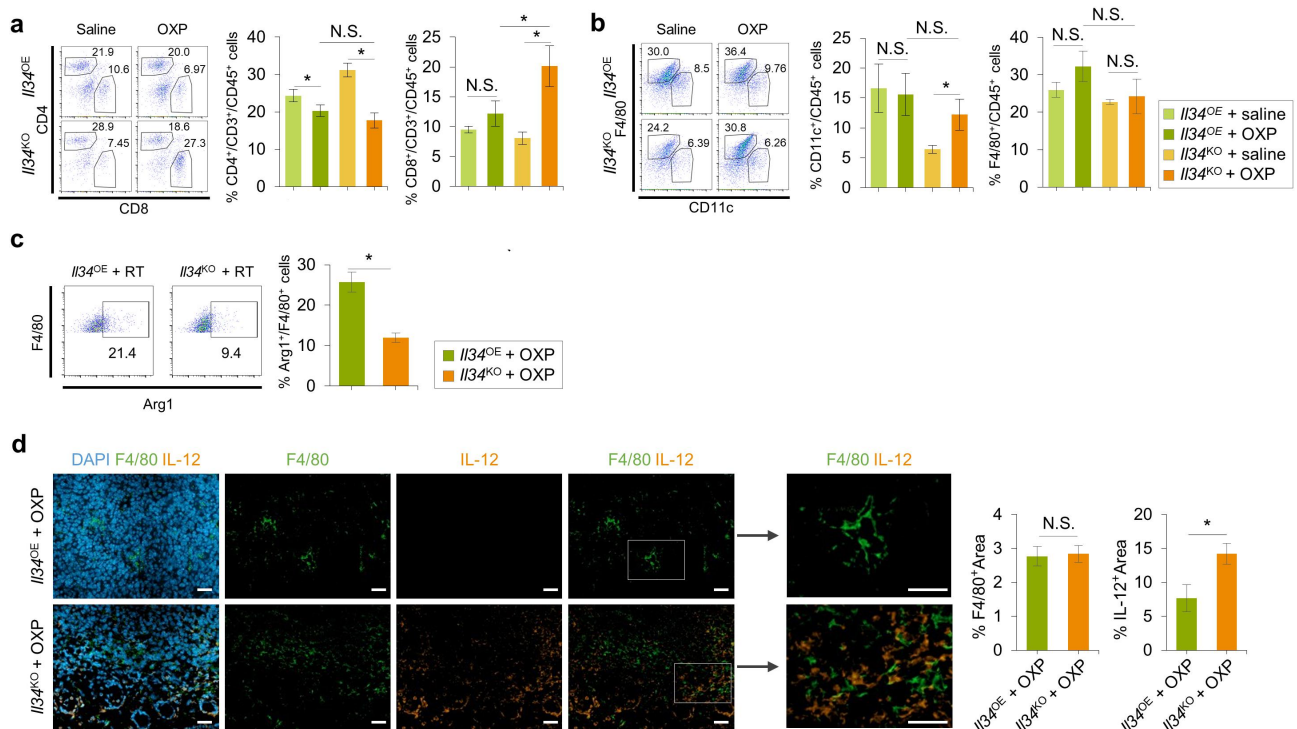


Figure 7. Characterization of IL-34-deficient and IL-34-expressing tumor microenvironment after chemotherapy. (a) Representative flow cytometry plots of T cells in tumor of *Il34^{KO}* and Mock 4T1 before and after chemotherapy with mean \pm SEM ($n = 6$ /group). (b) Representative flow cytometry plots of dendritic cells and macrophages in tumors of *Il34^{KO}* and Mock 4T1 before and after chemotherapy with mean \pm SEM ($n = 6$ /group). (c) Representative flow cytometry plots showing Arg1 expression of macrophages in tumors of *Il34^{KO}* and Mock 4T1 after chemotherapy with mean \pm SEM ($n = 4$ /group). (d) Representative images of IFN staining of *Il34^{KO}* and Mock 4T1 after chemotherapy. Bar graphs show the percentage of F4/80⁺ (left) and IL-12⁺ (right) areas with mean \pm SEM ($n = 10$ /group). Scale bar: 20 μ m, * $P < 0.05$; Tukey's multiple comparison test (a, b), Student's t-test (c, d), N.S., Not significant.

result with the IF analysis of the radiotherapy sample (Figure 4d), IL-12 expressing area increased significantly in $Il34^{KO}$ + OXP (Figure 7d). Finally, the anti-tumor effect of CSF-1 R inhibition in $Il34^{OE}$ + OXP was examined and compared to $Il34^{KO}$ + OXP. Anti-CSF-1 R was injected three and a day before the inoculation of $Il34^{OE}$ CT26 (Figure 8a). As expected, $Il34^{OE}$ + α -CSF-1 R + OXP showed the anti-tumor effect at the same level as $Il34^{KO}$ + OXP (Figure 8b).

Discussion

Previously, we reported that IL-34 reduces Nos2⁺ M1-biased macrophages in the immune-checkpoint-treated tumor micro-environment, which induces therapeutic resistance. As a follow-up study, we investigated the contribution of IL-34 inducing resistance against anti-tumor treatment such as radiotherapy or chemotherapy. In the case of the radiotherapy-treated tumors, unlike before the previous report,¹⁰ there was no difference in the proportion of Arg1⁺ and Nos2⁺ macrophages. The difference was identified by the expression of IL-12 instead of Arg1 and Nos2 expression. Similarly, the results of chemotherapy analysis showed the up-regulation of IL-12 expression in IL-34-deficient tumors. Our previous report also indicated the up-regulation of IL-12 family expression in the

tumor has an immunotherapeutic effect.¹⁰ Macrophages in the IL-34-deficient tumors after various treatments showed inflammatory properties despite the minor variations. Therefore, the therapeutic effects of various therapies in IL-34-deficient tumors suggest that due to an increase in IFN- γ ⁺ T cells, accompanied by an increase in pro-inflammatory macrophages in the tumor microenvironment.

The mechanism by which pro-inflammatory cytokine expressions, such as IL-12, are elevated in IL-34-deficient tumors remains unclear. The pro-inflammatory cytokines are known to be induced by the binding of DAMPs to TLR4 in immune cells.¹⁶ The expressions of *Hspa1a* and *Hmgb1*, which are known as DAMPs, have shown no differences between Mock + RT and $Il34^{KO}$ + RT (Figure 1d), and the protein expression of HMGB-1 also showed no differences (Supplementary figure S1a). This result suggests that something may influence by IL-34 acts as an inhibitory molecule in cells during the process of stimulation and expression of pro-inflammatory cytokines despite the same amount of stimulation from dying and damaged cells by radiotherapy. Therefore, it is necessary to illuminate how pro-inflammatory cytokine is suppressed in IL-34-expressing tumors stimulated by DAMPs.

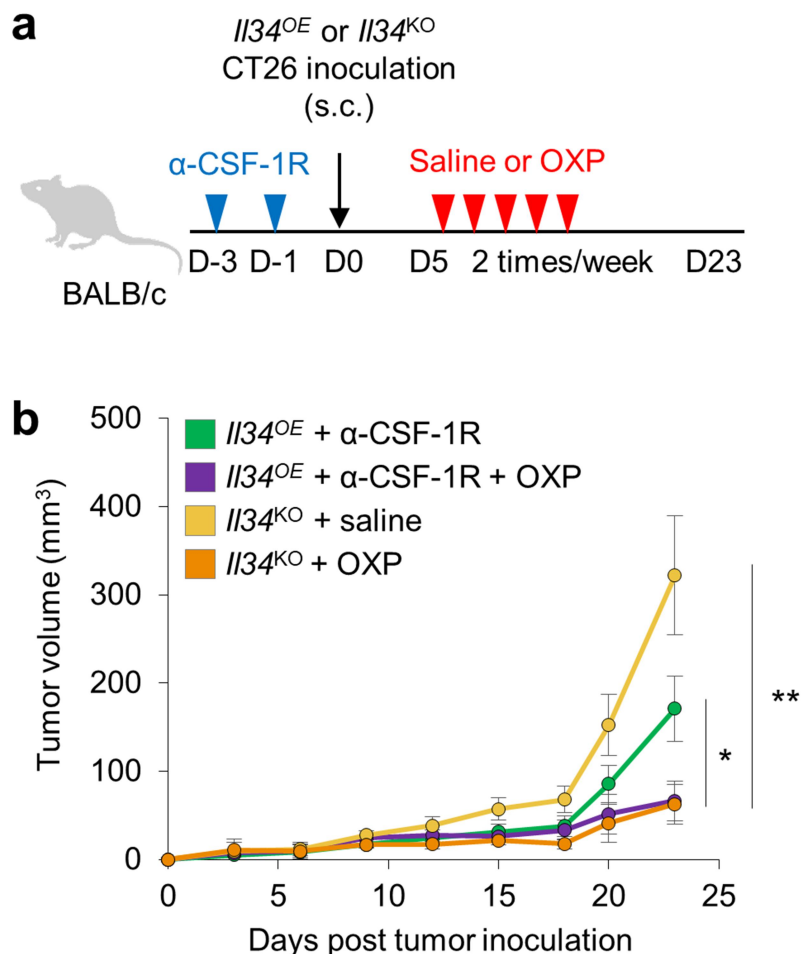


Figure 8. Evaluation of the possibility of improved treatment efficacy by CSF-1 R inhibition in OXP treatment. (a) the timeline of inoculation, irradiation, injection of anti-CSF-1 R antibody and analysis for OXP treatment. (b) Tumor volume of BALB/c mice until day 29 with mean \pm SEM ($n = 6$ /group). * $P < 0.05$, ** $P < 0.01$; Tukey's multiple comparison test, N.S., Not significant.

In this study, we observed improved response to X-ray radiation and Oxaliplatin chemotherapy in the IL-34-deficient tumors. It suggests that a combination of IL-34 inhibition and existing therapies, such as radiotherapy or chemotherapy for cancer that express IL-34 in a clinical trial may improve the therapeutic effect. Also, **Figures 5b and 8b** suggest that inhibition of CSF-1R may be a therapeutic approach in IL-34-expressing tumors in clinical trials. It has been reported that activation of the cGAS-STING pathway in tumor cells by radiotherapy induces IL-34 expression and immune-suppressive M2 macrophages. And inhibition of IL-34 was suggested to improve treatment by controlling the differentiation of macrophages in the article.¹⁷ In this study, we suggest IL-34 inhibition as an improved treatment with radiotherapy and chemotherapy. However, since we did not examine IL-34 inhibition experiments in the radiotherapy and chemotherapy model, it is worth considering as a follow-up study.

Acknowledgments

We thank all other members of Immunobiology laboratory for suggestions and technical assistance.

Disclosure statement

No potential conflict of interest was reported by the author(s).

Funding

This work was partly supported by research grants from the Ministry of Education, Culture, Sports, Science and Technology of Japan (#22K19449, K. Seino), Joint Research Program of the Institute for Genetic Medicine (K. Seino), the project of junior scientist promotion (K. Seino), and the Photo-excitonix Project in Hokkaido University (K. Seino).

ORCID

Ken-Ichiro Seino  <http://orcid.org/0000-0003-4122-1718>

Author contributions:

NH, HW, and KS designed the study. NH and TK performed experiments. All authors analyzed data and discussed the results. NH, HW, TK, RO, KS contributed to manuscript preparation. All authors reviewed the manuscript.

References

- Lin H, Lee E, Hestir K, Leo C, Huang M, Bosch E, Halenbeck R, Wu G, Zhou A, Behrens D, et al. Discovery of a cytokine and its receptor by functional screening of the extracellular proteome. *Science*. 2008;320(5877):807–811. doi:10.1126/science.1154370.
- Baghdadi M, Umeyama Y, Hama N, Kobayashi T, Han N, Wada H, Seino KI. Interleukin-34, a comprehensive review. *Journal of Leukocyte Biology query*. 2018;104(5):931–951. doi:10.1002/JLB.MR1117-457R.
- Uhlen M, Zhang C, Lee S, Sjöstedt E, Fagerberg L, Bidkhorji G, Benfiteas R, Arif M, Liu Z, Edfors F, et al. A pathology atlas of the human cancer transcriptome. *Science*. 2017;357(6352). doi:10.1126/science.aan2507.
- Baghdadi M, Endo H, Takano A, Ishikawa K, Kameda Y, Wada H, Miyagi Y, Yokose T, Ito H, Nakayama H, et al. High co-expression of IL-34 and M-CSF correlates with tumor progression and poor survival in lung cancers. *Sci Rep*. 2017;8(1):1–10. doi:10.1038/s41598-017-18796-8. 81. 2018.
- Zhou S-L, Hu Z-Q, Zhou Z-J, Dai Z, Wang Z, Cao Y, Fan J, Huang X-W, Zhou J. MiR-28-5p-IL-34-macrophage feedback loop modulates hepatocellular carcinoma metastasis. *Hepatology*. 2016;63(5):1560–1575. doi:10.1002/HEP.28445.
- Franzè E, Dinallo V, Rizzo A, Di Giovangiulio M, Bevivino G, Stolfi C, Caprioli F, Colantoni A, Ortenzi A, Di Grazia A, et al. Interleukin-34 sustains pro-tumorigenic signals in colon cancer tissue. *Oncotarget*. 2018;9(3):3432–3445. doi:10.18632/oncotarget.23289.
- Li CH, Chen ZM, Chen PF, Meng L, Sui WN, Ying SC, Xu AM, Han WX. Interleukin-34 promotes the proliferation and epithelial-mesenchymal transition of gastric cancer cells. *World J Gastrointest Oncol*. 2022;14(10):1968. doi:10.4251/WJGO.V14.I10.1968.
- Ségaly AI, Mohamadi A, Dizier B, Lokajczyk A, Brion R, Lanel R, Amiaud J, Charrier C, Boisson-Vidal C, Heymann D. Interleukin-34 promotes tumor progression and metastatic process in osteosarcoma through induction of angiogenesis and macrophage recruitment. *Int J Cancer*. 2015;137(1):73–85. doi:10.1002/IJC.29376.
- Han N, Baghdadi M, Ishikawa K, Endo H, Kobayashi T, Wada H, Imafuku K, Hata H, Seino K. Enhanced IL-34 expression in Nivolumab-resistant metastatic melanoma. *Inflamm Regen*. 2018;38(1). doi:10.1186/s41232-018-0060-2.
- Hama N, Kobayashi T, Han N, Yagita H, Baghdadi M, Seino K-I. Interleukin-34 Limits the Therapeutic Effects of Immune Checkpoint Blockade. 2020; doi:10.1016/j.isci.2020.101584.
- Lhuillier C, Rudqvist NP, Yamazaki T, Zhang T, Charpentier M, Galluzzi L, Dephore N, Clement CC, Santambrogio L, Zhou XK, et al. Radiotherapy-exposed CD8+ and CD4+ neoantigens enhance tumor control. *J Clin Invest*. 2021;131(5). doi:10.1172/JCI138740.
- Baghdadi M, Wada H, Nakanishi S, Abe H, Han N, Wira EP, Endo D, Watari H, Sakuragi N, Hida Y, et al. Chemotherapy-induced IL34 enhances immunosuppression by tumor-associated macrophages and mediates survival of chemoresistant lung cancer cells. *Cancer Res*. 2016;76(20):6030–6042. doi:10.1158/0008-5472.CAN-16-1170.
- Yamazaki T, Hannani D, Poirier-Colame V, Ladoire S, Locher C, Sistigu A, Prada N, Adjemian S, Catani JPP, Freudenberg M, et al. Defective immunogenic cell death of HMGB1-deficient tumors: compensatory therapy with TLR4 agonists. *Cell Death Differ*. 2014;21(1):69–78. doi:10.1038/CDD.2013.72.
- Mirlekar B, Pylayeva-Gupta Y. IL-12 family cytokines in cancer and immunotherapy. *Cancers Basel*. 2021;13(2):1–23. doi:10.3390/CANCERS13020167.
- Gou HF, Huang J, Shi HS, Chen XC, Wang YS, Mattei F. Chemoimmunotherapy with Oxaliplatin and interleukin-7 inhibits colon cancer metastasis in mice. *PLoS One*. 2014;9(1):e85789. doi:10.1371/JOURNAL.PONE.0085789.
- Jang GY, Won LJ, Kim YS, Lee SE, Han HD, Hong KJ, Kang TH, Park YM. Interactions between tumor-derived proteins and Toll-like receptors. *Experimental & Molecular Medicine*. 2020;52(12):1926–1935. 5212. 2020. doi:10.1038/s12276-020-00540-4.
- Nakajima S, Mimura K, Kaneta A, Saito K, Katagata M, Okayama H, Saito M, Saze Z, Watanabe Y, Hanayama H, et al. Radiation-induced remodeling of the tumor microenvironment through tumor cell-intrinsic expression of Cgas-STING in esophageal squamous cell carcinoma. *Int J Radiat Oncol*. 2022 Nov 8;115(4):957–971. doi:10.1016/j.IJROBP.2022.10.028.